NJC

New Journal of Chemistry

An international journal of the chemical sciences

www.rsc.org/njc

Volume 32 | Number 6 | June 2008 | Pages 893–1080

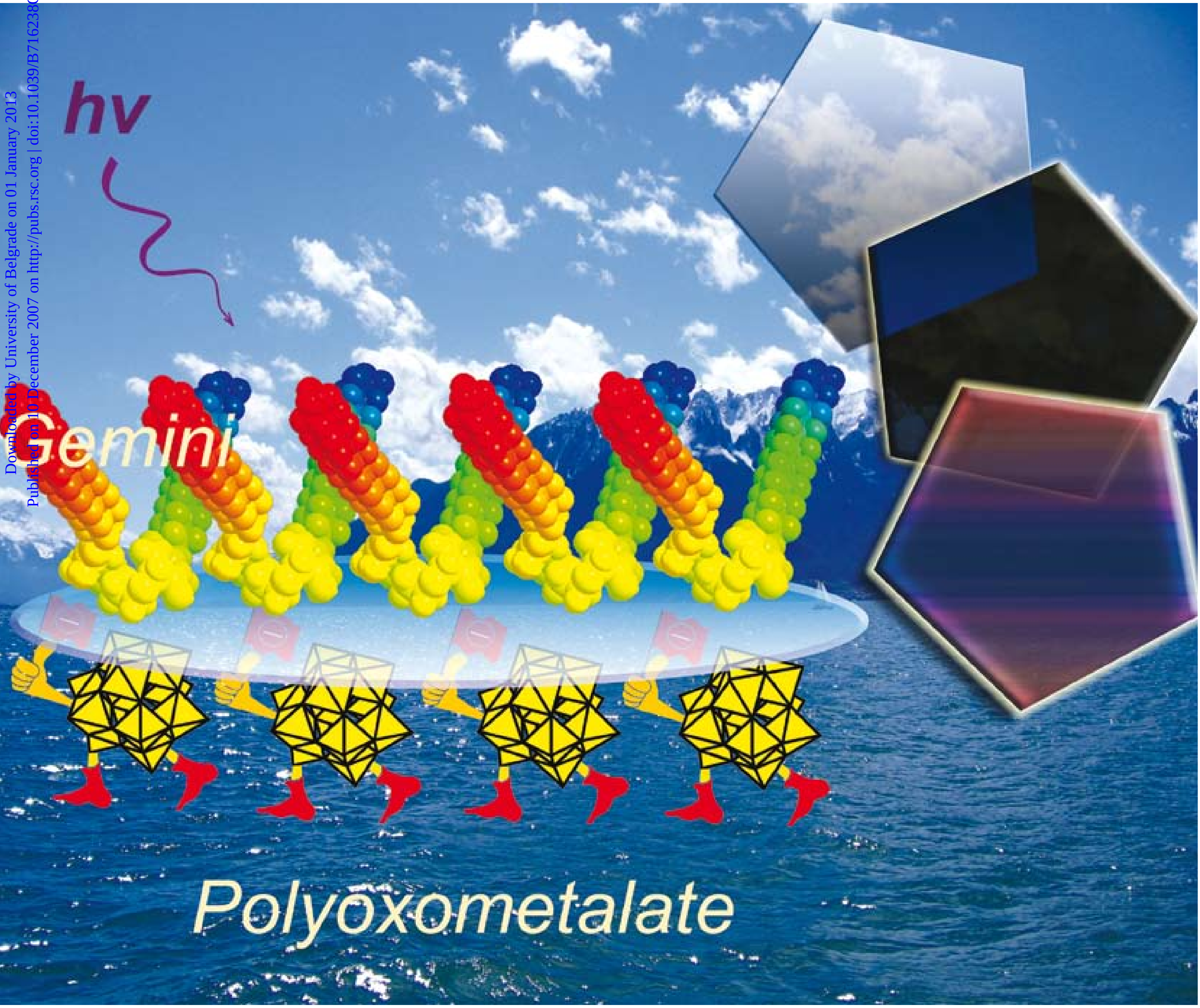

ISSN 1144-0546

RSC Publishing

CENTRE NATIONAL
DE LA RECHERCHE
SCIENTIFIQUE

PAPER
Min Jiang, Tifeng Jiao and Minghua Liu
Photochromic Langmuir–Blodgett films based on polyoxomolybdate and gemini amphiphiles

Photochromic Langmuir–Blodgett films based on polyoxomolybdate and gemini amphiphiles†‡

Min Jiang, Tifeng Jiao and Minghua Liu*

Received (in Montpellier, France) 22nd October 2007, Accepted 26th November 2007
First published as an Advance Article on the web 10th December 2007
DOI: 10.1039/b716238c

Novel photochromic hybrid organized molecular films composed of polyoxomolybdate (PMo_{12}) and a series of gemini amphiphile (BisBC18Nn, n = 1, 2, 3) with different hydrophilic spacer length were fabricated by the Langmuir–Blodgett (LB) technique. When these gemini amphiphiles were spread on an aqueous PMo_{12} subphase, hybrid monolayers were formed *in situ* at the air/water interface through electrostatic interaction. These hybrid monolayers were subsequently transferred onto solid substrates and characterized by UV-Vis spectroscopy, Fourier-transform infrared spectroscopy (FT-IR), X-ray diffraction (XRD), atomic force microscopy (AFM) and cyclic voltammetry (CV). The hybrid multilayer films showed photochromic property, *i.e.*, the color of BisBC18Nn/PMo_{12} hybrid films changed from pale yellow to cyan under UV irradiation and decoloration occurred when the films were heated in the air. Such processes could be repeated many times and the films exhibited excellent photochromic reversibility. A slight difference in the coloration of the hybrid films with different spacer lengths was observed.

Introduction

Photochromism, which was first discovered in 1876, is regarded as a reversible transformation in the molecular structure or charge distribution during light irradiation.[1–3] Over the more than one hundred years since, there have been a large number of researchers interested in the photochromic materials in view of their potential applications in several important areas, such as high-density optical storage, optical switching, image processing, chemical sensors and so on.[4–6] Most attention has been paid to four photochromic systems including azobenzenes,[7] spiropyrans,[8] fulgides[9] and diarylethenes.[10] Upon ultraviolet irradiation, the *cis–trans* isomerization of a N=N bond, dissociation of a C–O bond, the bond rearrangement and electrocyclic reactions were suggested to be responsible of photochromism in these systems, respectively. Besides these organic molecules, some inorganic compounds also exhibited photochromism.[11] Polyoxometalates (POMs) are typical inorganic metal oxide clusters with a wealth of topologies, chemical and physical properties, and have been used in some fields such as catalysis, medicine and materials science.[12] As versatile inorganic entities for the construction of functionally active solids, POMs can accept electrons or protons to become coloured mixed-valence species while retaining their structural integrity, which make them suitable for photochromic and electrochromic materials.[13] Incorporation of POMs into organic or hybrid organic–inorganic materials led to photoresponsive systems, whose properties were manipulated by light. Especially, alkylammonium polyoxomolybdates have been found to be photosensitive as solids and in solutions.[13a,14] When alkylammonium polyoxomolybdates were irradiated by UV light at a wavelength corresponding to the O → Mo ligand-to-metal charge transfer (LMCT), the white crystals became reddish brown or violet because some Mo^{6+} were reduced to Mo^{5+}. To date, several strategies have been adopted to obtain POM-based photochromic materials, including layer-by-layer method,[14a,15] sol–gel method[14b,16] and cast technique.[14c,17] The Langmuir–Blodgett (LB) technique is a useful method for controlling and modifying photochromic reaction by organizing reactive molecules intentionally in the solid state,[7a,c,8a,b,10a,18] and provides the possibility to fabricate a well-defined hybrid film.

Gemini amphiphiles are a group of amphiphiles consisting of two hydrocarbon chains linked together by two ionic groups and a hydrocarbon spacer group.[19] They have a wealth of variable parameters such as the length of hydrophobic chains, the size of hydrophilic groups, the type of counterions and the flexibility and polarity of the spacer, which can provide a good modulation on the interfacial properties.[20] The effect of spacer length is one of the most interesting properties which can control the separation between the headgroups and thus influence the molecular assembly, the stability and topography of the aggregates. In our previous papers, the hydrophobic spacer was used to regulate the surface properties of the Langmuir monolayer and the nanoarchitectures formed by the gemini amphiphiles themselves and the hybrid films of the gemini amphiphiles with organic dyes, DNA and POMs.[21]

In the present paper, we extended our work to hybrid organized molecular films of a series of gemini amphiphiles

---

Beijing National Laboratory for Molecular Sciences (BNLMS), CAS Key Laboratory of Colloid and Interface Science, Institute of Chemistry, The Chinese Academy of Sciences, CAS, Beijing, 100080, P. R. China. E-mail: liumh@iccas.ac.cn

† The HTML version of this article has been enhanced with colour images.

‡ Electronic supplementary information (ESI) available: Fig. S1: π–A isotherms of gemini amphiphiles BisBC18Nn on the subphase of pure water. Fig. S2: Coloration–decoloration cycles of BisBC18Nn/PMo_{12} films at 700 nm. Fig. S3: FTIR spectra of BisBC18Nn/PMo_{12} multilayer films before irradiation, after irradiation and after heating. See DOI: 10.1039/b716238c

with imine-containing hydrophilic spacers of different length and polyoxomolybdates fabricated by the LB technique. Transferred multilayer films were characterized by UV-Vis spectroscopy, AFM, XRD, CV and FT-IR spectroscopy. The results suggested that the hybrid films had well-defined layer structures and exhibited good reversibility of photochromism. Extending the length of the hydrophilic spacer from one to three imine groups could cause different interfacial behavior of monolayer films, regular changes of electrochemical behavior of PMo_{12} and a slight differences in the photochromic properties of the hybrid films.

Experimental

Materials

The Keggin-type phosphomolybdic acid, $H_3PMo_{12}O_{40}$ (abbreviated as PMo_{12}), was synthesized according to the literature procedure.[22] A series of gemini amphiphiles, *N*,*N*′-bis(4-octadecyloxysalicylidene)diethylene triamine (BisBC18N1), *N*,*N*′-bis(4-octadecyloxysalicylidene)triethylene tetramine (BisBC18N2) and *N*,*N*′-Bis(4-octadecyloxysalicylidene)tetraethylene pentamine (BisBC18N3), were synthesized according to the recent report.[23] The final products were confirmed by mass spectra and ^{1}H NMR as well as elemental analysis. The molecular structures are shown in Fig. 1. Chloroform was purchased from Beijing Chemicals and distilled before use. Pure water (18 MΩ cm) was obtained from the Milli-Q system and used in all cases.

Preparation

The chloroform solutions of BisBC18N*n* ($n = 1, 2, 3$) with a concentration of 0.5 mM were spread onto 0.1 mM PMo_{12} using an aqueous subphase. After complete evaporation of the solvent for 15 min, the surface pressure–area isotherms (π–A) were recorded by compressing the barrier at a constant speed of 7.5 cm^2 min^{-1}. A vertical dipping method was employed to obtain a one-layer LB film with an upstroke speed of 2 mm min^{-1} and the LB monolayers were transferred onto freshly cleaved mica for AFM measurement. The hybrid multilayers were transferred at 20 mN m^{-1} by a Langmuir–Sächffer (LS) horizontal lifting method onto hydrophilic substrates: quartz plates for UV-Vis spectroscopy and XRD measurements, CaF_2 slides for FT-IR spectroscopy measurements, and indium tin oxide (ITO) glass slides for CV measurements.

Characterization

The π–A isotherm measurements and LB film preparation were operated on a computer-controlled Langmuir trough (KSV 1100, Helsinki, Finland) with an area of 75 × 325 mm^2. The working temperature of the water in the trough was controlled within 20.0 ± 0.2 °C by circulating thermostated water. AFM images were recorded on a Digital Instrument Nanoscope IIIa Multimode system (Santa Barbara, CA) with a silicon cantilever using the tapping mode. UV-Vis and FT-IR spectra were recorded on a JASCO V-530 spectrometer and FT-IR 660 spectrophotometer, respectively. Low-angle XRD of LB multilayer films was performed on a Hitachi National D/Max-RB X-ray diffractometer with Cu-Kα radiation. Electrochemical experiments were carried out on a Model 600B Voltammetric Analyzer (CHI Instruments, USA) in a conventional one-compartment cell with ITO as working electrode, Ag/AgCl as reference electrode and a Pt wire as an auxiliary electrode. All electrochemical measurements were carried out at room temperature under nitrogen atmosphere. Photochromic experiments were carried out using a 500 W mercury lamp ($\lambda = 365$ nm) as the light source. The distance between the lamp and the sample was 20 cm. Samples were kept in air during irradiation.

Results and discussion

1 Formation of hybrid monolayers at the air/aqueous PMo_{12} interface

π–A isotherms of the spreading films. The π–A isotherms of the spreading films of BisBC18N*n* ($n = 1, 2, 3$) on the subphase of an aqueous PMo_{12} solution are presented in Fig. 2. In comparison with the isotherms of BisBC18N*n* on a pure water surface (see ESI,‡ Fig. S1), the isotherms of the corresponding amphiphiles on the PMo_{12} subphase all showed increases in molecular area. This may be the result of the hydrophilic spacer (in our previous report, the molecular areas of the gemini amphiphile with hydrophobic spacer on polyoxometalate subphase were smaller than that on the pure water surface).[21c] Since the PMo_{12} solution is acidic with pH = 3, it can make the –NH– group in BisBC18N*n* protonated. Therefore, the strong interaction between positively charged amphiphiles and negatively charged PMo_{12} resulted in spontaneous formation of stable monolayers. For the BisBC18N*n* ($n = 1, 2, 3$) molecules, their isotherms on a pure water surface were nearly overlapped (see ESI,‡ Fig. S1), while their isotherms on the PMo_{12} subphase exhibited obvious

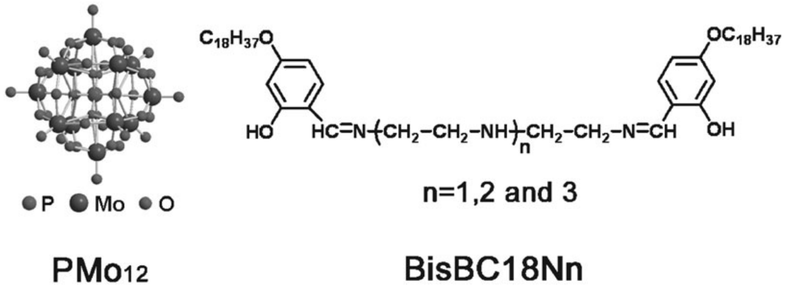

Fig. 1 Structures of phosphomolybdic acid PMo_{12} and gemini amphiphiles BisBC18N*n* ($n = 1, 2, 3$).

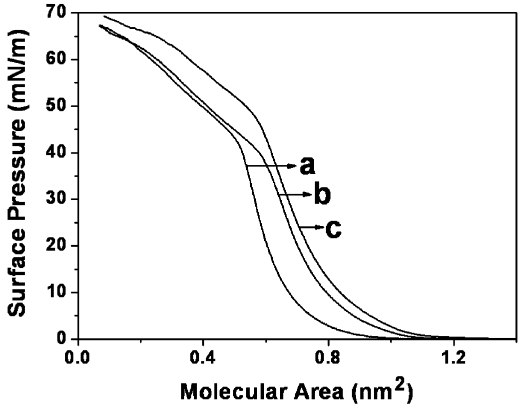

Fig. 2 π–A isotherms of gemini amphiphiles: (a) BisBC18N1, (b) BisBC18N2, (c) BisBC18N3 on the subphase of PMo_{12} aqueous solution.

differences. With an increase in the number of diethylene amine groups, the limiting molecular area of the corresponding gemini amphiphile became larger: 0.70, 0.81 and 0.84 nm^2 molecule^{-1}, respectively, as a consequence of hydrophilic chain extension. The three BisBC18Nn/PMo_{12} (n = 1, 2, 3) isotherms all showed transition points between 40 and 50 mN m^{-1}. Such phenomena could be related to a phase transition from an expanded state to a condensed liquid phase. Moreover, the limiting surface areas were different from the lift-off areas, which proved that these gemini amphiphiles had large compressibility.

AFM characterization. To properly understand the interaction between gemini amphiphiles and polyoxomolybdate at the air/water surface, and the effect of hydrophilic spacer length on the interfacial behaviour of gemini amphiphile, the morphologies of one-layer LB films were investigated by AFM measurement. On the whole, uniform domains with different sized holes were observed in one-layer BisBC18Nn/PMo_{12} (n = 1, 2, 3) films (as shown in Fig. 3). On analyzing the height profiles of the BisBC18N1/PMo_{12} monolayer film, it was found that the height of the holes was 1.3 nm. In the case of BisBC18N2/PMo_{12} and BisBC18N3/PMo_{12} film, the holes were about 1.5 and 1.7 nm in depth, respectively. Comparing these images of the three BisBC18Nn/PMo_{12} monolayers transferred at the same pressure, we observed that the net-like domains became more distinct and the mean roughness of the surface rose with increase of hydrophilic spacer length. According to the height of the holes, the domains should be composed with one layer of BisBC18Nn molecules, with the PMo_{12} layer situated beneath the BisBC18Nn domains.

2 Characterization of transferred multilayer films

X-Ray diffraction. The layered nature of the deposited films was established by X-ray diffraction. Good patterns extending to second-order diffraction were observed for these LB films, as shown in Fig. 4. The layer distances (d-spacing) of the films were calculated based on the Bragg equation ($n\lambda = 2d\sin\theta$). The d-spacings were estimated to be 3.76, 3.71 and 3.74 nm for the BisBC18Nn/PMo_{12} (n = 1, 2, 3) hybrid films, respectively. From these experimental values, it could be regarded that all the films were Y-type multilayers and each unit was composed of two-layer gemini amphiphiles and one layer of PMo_{12}. The alkyl chains were tilted from the vertical array and intercrossed between two-layer gemini amphiphiles, which was different from the arrangement of long alkyl chains in other Y-type LB films made of typical amphiphiles and POMs.[24] Possible structure models are given in Fig. 4(d).

Cyclic voltammetry. In the previous results, it was found that the length of hydrophobic spacer could affect the electrochemical behaviour of the immobilized heteropolyanions.[25] We wondered if the length of hydrophilic spacers had the same influence as hydrophobic spacers on the electrochemical behaviour of PMo_{12}. The electrochemical response of the three-layer BisBC18Nn/PMo_{12} (n = 1, 2, 3) films are shown in Fig. 5. Three well-defined sets of reversible peaks were observed in each hybrid films, which corresponded to reversible one-, one- and two-electron reduction processes of PMo_{12}.[22,26] In addition, the peak potential separations of three pairs ΔE_p ($\Delta E_p = E_{pa} - E_{pc}$; E_{pa} and E_{pc} are the anodic and cathodic peak potential, respectively) were <20 mV *cf.* the zero value expected for a reversible surface redox process.[27] This might be attributed to a non-ideal behaviour of the adsorbed

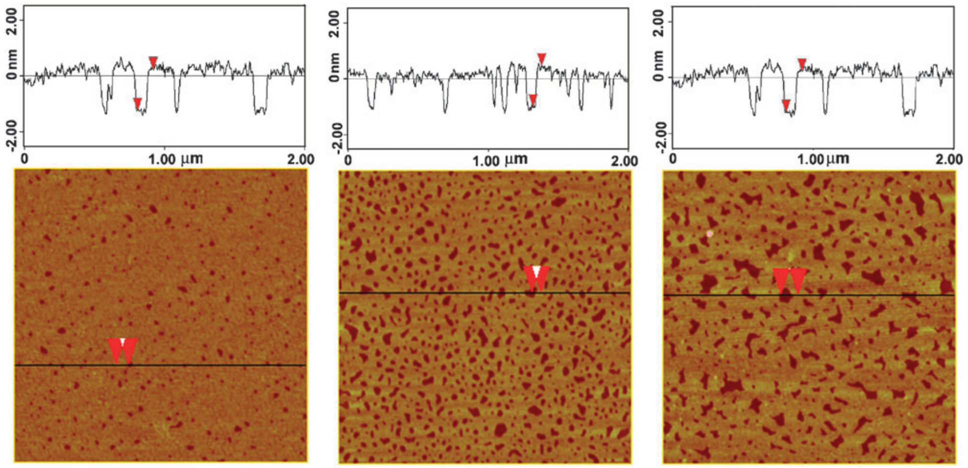

Fig. 3 AFM images of one-layer films transferred at 20 mN m^{-1}: (a) BisBC18N1/PMo_{12}, (b) BisBC18N2/PMo_{12}, (c) BisBC18N3/PMo_1.

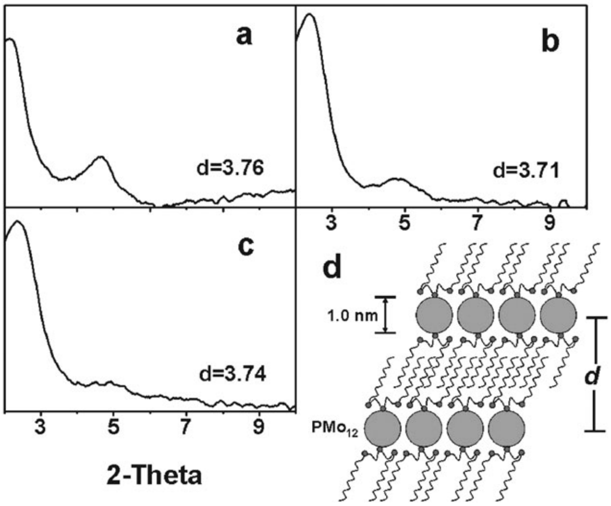

Fig. 4 XRD patterns of multilayer films of (a) BisBC18N1/PMo_{12}, (b) BisBC18N2/PMo_{12} and (c) BisBC18N3/PMo_{12} transferred at 20 mN m^{-1}. (d) Schematic representation of a possible structure of BisBC18N*n*/PMo_{12} hybrid films.

moieties, which is a common phenomenon in all electrodes coated at the monolayer or submonolayer level.[28] With the spacer length increasing, E_{pc2} slightly shifted to larger potential (from curve (a) to (c)). This indicated that the participation of more hydrophilic groups of gemini amphiphiles made the reduction process of the PMo_{12} easier. This result is opposite to the conclusion that more hydrophobic spacers do not benefit the reduction process of the PW_{12}.[25]

UV-Vis spectra. Fig. 6 shows the UV-Vis spectra of BisBC18N*n*/PMo_{12} (n = 1, 2, 3) multilayer films transferred at a constant surface pressure of 20 mN m^{-1}. The absorption bands at 231, 275 and 302 nm were designated as π–π* and n–π* transitions for electrons localized on the azomethine group.[23] However, only the band at 320 nm and the shoulder band at 220 nm could be observed in the BisBC18N*n*/PMo_{12} (n = 1, 2, 3) multilayer films. Two characteristic bands of PMo_{12} in solution are at 215 and 330 nm corresponding to the different oxygen to molybdenum charge transfer (CT) transitions.[14c] Therefore, we concluded that the shoulder band at 220 nm was a result of the overlap of two bands (at 215 and 231 nm), while the band at 320 nm corresponded to the overlap of bands at 302 and 330 nm. Such characteristics of absorption bands may be attributed not only to the coexistence of PMo_{12} and BisBC18N*n* molecules, but also to the ordered arrangement of the molecules.

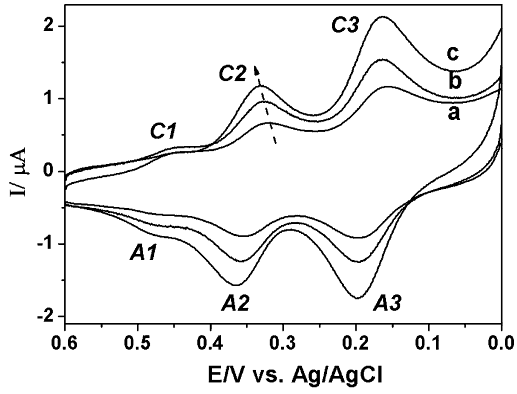

Fig. 5 CVs of three-layer films modified on ITO in 0.5 mol L^{-1} H_2SO_4 solution: (a) BisBC18N1/PMo_{12}, (b) BisBC18N2/PMo_{12}, (c) BisBC18N3/PMo_{12}; scan rate: 50 mV s^{-1}, initial potential: 0 V.

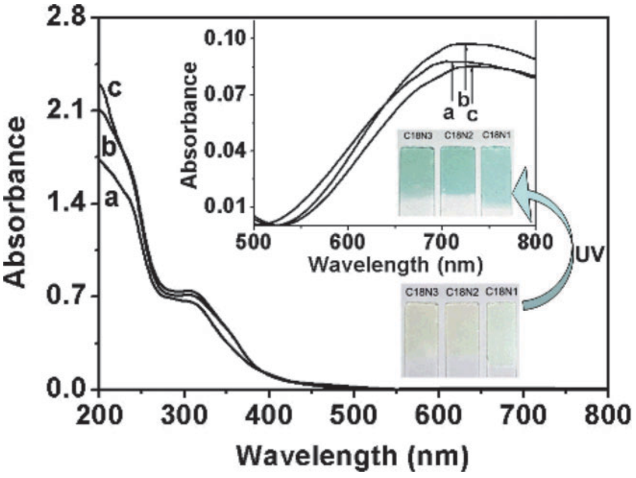

Fig. 6 UV-Vis absorption spectra of 70-layer multilayer films transferred at a constant pressure of 20 mN m^{-1}: (a) BisBC18N1/PMo_{12}, (b) BisBC18N2/PMo_{12}, (c) BisBC18N3/PMo_{12}. The inset shows UV-Vis spectra of the corresponding films after irradiation.

FT-IR spectra. FT-IR spectroscopy has been widely utilized to detect changes of molecular structure and orientation in organized films. FT-IR spectra of BisBC18N*n*/PMo_{12} (n = 1, 2, 3) multilayer films in the region from 900 to 3000 cm^{-1} before and after irradiation are presented in the ESI,‡ Fig. S3, with main vibration bands in the FT-IR spectra listed in Table 1. In the as-deposited films the symmetric and asymmetric vibrations of CH_2 were observed at 2850 and 2918 cm^{-1}, respectively, which indicated that the hydrocarbon chains were highly ordered.[29] The strong bands at *ca.* 950 and 1065 cm^{-1} were associated with the vibration modes of $Mo{=}O_d$ and $P–O_a$ stretching band, respectively.[12a,30] In the hybrid films, these bands narrowed and slightly shifted in contrast with the bands in a KBr pellet. The result showed that PMo_{12} clusters might have a particular orientation in the multilayer films prepared using the LB technique. Alternatively, it may be the result of strong Coulombic interaction between PMo_{12} anions and amphiphile cations. Further strong vibration bands at 1606 (1607, 1609), 1465 (1465, 1465) and 1296 (1296, 1296) cm^{-1} were ascribed to the vibrations of the C=N bond, and the scissor vibrations of the CH_2 and phenolic group, respectively. When the gemini amphiphiles with different hydrophilic spacer length interacted with the PMo_{12} cluster, two characteristic bands of PMo_{12} in the corresponding hybrid films showed differences in peak positions and relative intensities. Actually the relative intensity of $Mo–O_d$ stretching band with respect to the $P–O_a$ vibration may be directly correlated with electrostatic interaction between the amphiphile and PMo_{12}. With an increase in the hydrophilic spacer length the relative intensity became

Table 1 Characteristic vibration bands of three hybrid films in different conditions

	BisBC18N1/PMo_{12}			BisBC18N2/PMo_{12}			BisBC18N3/PMo_{12}		
IR band/cm^{-1}	Original	Light	Heat	Original	Light	Heat	Original	Light	Heat
CH_2 (asym)	2918	2919	2921	2918	2920	2922	2918	2920	2922
CH_2 (sym)	2850	2850	2850	2850	2850	2850	2850	2850	2850
$P{=}O_a$	1060	1054	1057	1063	1055	1060	1064	1056	1060
$Mo–O_d$	950	942	945	951	944	947	951	943	947
$I_{Mo-O_d}/I_{P=O_a}$[a]	0.5	1.7	1.2	0.6	2.8	1.6	0.7	2.7	1.7

[a] Intensity ratio of $Mo–O_d$ to $P{=}O_a$ vibration band.

stronger due to more $–NH_2^+–$ groups interacting with the PMo_{12} cluster, which resulted in a stronger electrostatic interaction.

3 Photochromic properties of the hybrid films

Initially, these multilayer films were perfectly transparent in the visible range (digital photo shown in Fig. 6). After UV irradiation for 10 min, a strong absorption band with a maximum at approximately 700 nm can be observed in the inset of Fig. 6. Such an absorbance (0.09 at 700 nm) was sufficient to allow visual perception of the photochromic coloration and is characteristic of coloured, reduced molecular species (so-called heteropoly blues)[30] with d–d band charge transfer intervalence transitions ($Mo^{6+} \rightarrow Mo^{5+}$) in the visible region. The color of the BisBC18N*n*/PMo_{12} multilayer films changed from very pale yellow to cyan. The position of maximum absorbance showed a small red shift with an increase of hydrophilic spacer length (see arrows in inset to Fig. 6). Furthermore, the reaction kinetics of coloration and decoloration were studied. Fig. 7(a) shows the change of the absorbance of the multilayer at 700 nm with irradiation time. In the first 5 min, the change of absorbance was distinct for these hybrid films. After irradiation for 15 min, the BisBC18N2/PMo_{12} and BisBC18N3/PMo_{12} films nearly reached saturation, while BisBC18N1/PMo_{12} films seemed not to reach saturation even after 20 min irradiation. The cyan-coloured films were found to be stable in N_2 atmosphere. According to previous research, a bleaching process could occur in the presence of O_2[13a,14] but in our case the response speed was very slow and the bleaching process typically took around ten days in air at room temperature. Heating, however, led to fast and homogeneous bleaching of the cyan-coloured films in the presence of oxygen. Fig. 7(b) shows the decoloration process with heating time at 100 °C in air. The bleaching speed of coloured BisBC18N1/PMo_{12} was faster than that of the other two films. Based on the above results, it was confirmed that BisBC18N3/PMo_{12} films exhibited the poorest response to photochromic reaction and the hybrid films with shorter spacers tended to show better photochromic ability. This suggested that the photochromic behaviour of polyoxomolybdates could be improved by choosing appropriate organic components.

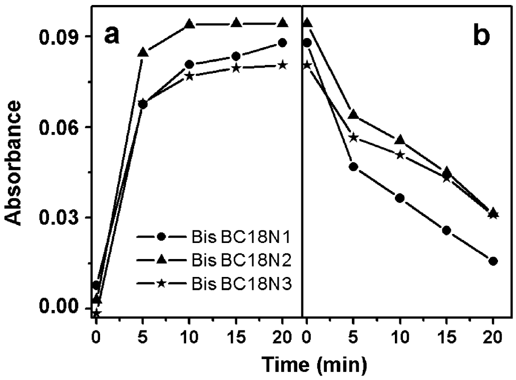

Fig. 7 (a) Plot of the absorbance at 700 nm with irradiation time. (b) Plot of the absorbance at 700 nm with heating time in the presence of O_2.

Repeated irradiation and heating cycles of multilayers revealed the photochromic reversibility (see ESI,‡ Fig. S2). After tens of cycles, no clear photofatigue of photochromic behaviour were observed. In other words, three hybrid films presented good coloration–decoloration reversibility. The response time of the photochromic reaction was dependent on the power of the irradiation source with a 30 W UV lamp leading to a slower coloration process.

There were three important phenomena under irradiation and heat revealed from FT-IR spectra of these films. Firstly, the frequency of the asymmetric CH_2 stretching bands of the hydrocarbon chains shifted from 2918 to 2919 or 2920 cm^{-1} in the coloured film, and continued to show a shift further to higher frequency after heating. If the coloured film was kept in the air without heating for a long time, the position of CH_2 vibration bands in the bleached film gradually recovered to 2918 cm^{-1}. The frequencies of CH_2 stretching bands are sensitive to the conformation of a hydrocarbon chain with lower frequencies of bands characteristic of highly ordered alkyl chains, while shifts to higher wavenumber are indicative of an increase in conformational alkyl disorder. In other words, irradiation and heating could cause the disordering of the alkyl chains. Secondly, the vibrational bands of $P–O_a$ and $Mo–O_d$ shifted to lower frequency under irradiation. When heated in the air, these bands of the films returned back to their original values to some extent. In general, the position of $Mo–O_d$ stretches changes with electrostatic interaction. The shift to low wavenumber of the $Mo–O_d$ asymmetrical stretching frequency of the composite film occurred because irradiation shortens the anion–anion distances and enhanced the electrostatic interaction. By contrast, heating lengthened the distances and weakened the interaction. Third, the ratio of the intensities of the $Mo–O_d$ to $P–O_a$ band increased under irradiation and decreased under heating, which further proved that irradiation enhanced the interaction between the amphiphile and PMo_{12} while heat weakened this interaction. Under stimulation of light and heat, the BisBC18N1/PMo_{12} multilayer films presented the smallest change of the ratio of the intensities of Mo–O_d to P–O_a band during the coloration and decoloration process, while BisBC18N3/PMo_{12} multilayer films showed the greatest changes. On the whole, the PMo_{12} molecules retained their basic structure after coloration except for some distortion, with such a distortion contributing to the transformation of the bonds between the polyoxomolybdates and the amphiphile.

With the increase of hydrophilic spacer length, more amine groups are anchored on the surface of PMo_{12} so that the electrostatic interaction between BisBC18N*n* and PMo_{12} is enhanced. Therefore, BisBC18N3/PMo_{12} multilayer films showed the greatest changes in the relative intensity of the Mo–O_d to P–O_a band during the coloration and decoloration process. However, more strong electrostatic interaction will act against proton transfer during the photochromic process,[13*a*] which causes the slowest response of BisBC18N3/PMo_{12} films to photochromic reaction. On the contrary, the weakest interaction between BisBC18N1 and PMo_{12} benefited the hybrid film which showed the best photochromic ability.

Conclusions

Hybrid multilayer films based on a series of gemini amphiphiles BisBC18N*n* (n = 1, 2, 3) with different hydrophilic spacer lengths with phosphomolybdic acid (PMo_{12}) were constructed through the LB technique. The hybrid monolayers could be deposited as multilayer films and all the hybrid films exhibited a well-defined layer structure. When exposed to UV light, the BisBC18N*n*/PMo_{12} hybrid films changed from pale yellow to cyan. The reverse reaction occurred in air or O_2 with the help of heat. Repeatable coloration–decoloration proved the excellent photochromic reversibility of the hybrid films. Although the spacer length of the gemini amphiphiles has an obvious effect on the monolayer property, it affects the photochromic properties only slightly. The spacer length causes slight differences in the maximum absorption position of the coloured species, which may be due to subtle change of the environment around the POM. By analyzing changes in the position and relative strength of Mo–O_d and P–O_a stretching band, it was revealed that BisBC18N1/PMo_{12} hybrid films with the shortest spacer showed the best photochromic ability. The present results prove that an appropriate selection of the polyoxometalate and amphiphiles could lead to the preparation of hybrid LB films that exhibit good photochromic properties.

Acknowledgements

This work was supported by the National Natural Science Foundation of China (No. 20533050 and 90306002) and the Fund of the Chinese Academy of Sciences.

References

1 E. ter Meer, *Justus Liebigs Ann. Chem.*, 1876, **181**, 1.
2 R. Exelby and R. Grinter, *Chem. Rev.*, 1965, **65**, 247.
3 G. H. Brown, *Photochromism*, Wiley-Interscience, New York, 1971.
4 J. A. Delaire and K. Nakatani, *Chem. Rev.*, 2000, **100**, 1817.
5 *Photochromism Molecules and Systems*, ed. H. Dürr and H. Bouas-Laurent, Elsevier, Amsterdam, 1990.
6 M. Irie, in *Photoreactive Materials for Ultrahigh-Density Optical Memory*, Elsevier, Amsterdam, 1994.
7 (*a*) W. S. Xia, C. H. Huang, X. Z. Ye, C. P. Luo, L. B. Gan and Z. F. Liu, *J. Phys. Chem.*, 1996, **100**, 2244; (*b*) Z. Sekkat, J. Wood, Y. Geerts and W. Knoll, *Langmuir*, 1995, **11**, 2856; (*c*) J. Stumpe, T. Fischer and H. Menzel, *Macromolecules*, 1996, **29**, 2831; (*d*) M. Matsumoto, S. Terrettaz and H. Tachibana, *Adv. Colloid Interface Sci.*, 2000, **87**, 147; (*e*) Y. Einaga, R. Mikami, T. Akitsu and G. M. Li, *Thin Solid Films*, 2005, **493**, 230; (*f*) T. Enomoto, H. Hagiwara, D. A. Tryk, Z. F. Liu, K. Hashimoto and A. Fujishima, *J. Phys. Chem. B*, 1997, **101**, 7422; (*g*) M. Matsumoto, D. Miyazaki, M. Tanaka, R. Azumi, E. Manda, Y. Kondo, N. Yoshino and H. Tachibana, *J. Am. Chem. Soc.*, 1998, **120**, 1479; (*h*) H. Sakai, Y. Orihara, H. Kodashima, A. Matsumura, T. Ohkubo, K. Tsuchiya and M. Abe, *J. Am. Chem. Soc.*, 2005, **127**, 13454.
8 (*a*) H. Tachibana, Y. Yamanaka and M. Matsumoto, *J. Phys. Chem. B*, 2001, **105**, 10282; (*b*) E. Ando, K. Moriyama, K. Arita and K. Morimoto, *Langmuir*, 1990, **6**, 1451; (*c*) J. Z. Zhang, B. J. Schwartz, J. C. King and C. B. Harris, *J. Am. Chem. Soc.*, 1992, **114**, 10921; (*d*) J. Hibino, K. Moriyama, M. Suzuki and Y. Kishimoto, *Thin Solid Films*, 1992, **210**, 562; (*e*) S. Benard and P. Yu, *Adv. Mater.*, 2000, **12**, 48; (*f*) H. Tomioka and T. Itoh, *J. Chem. Soc., Chem. Commun.*, 1991, 532.
9 (*a*) Y. Yokoyama, *Chem. Rev.*, 2000, **100**, 1717; (*b*) Y. Liang, A. S. Dvornikov and P. M. Rentzepis, *Macromolecules*, 2002, **35**, 9377; (*c*) A. Santiago and R. S. Becker, *J. Am. Chem. Soc.*, 1968, **90**, 3654; (*d*) C. Lenoble and R. S. Becker, *J. Phys. Chem.*, 1986, **90**, 2651; (*e*) H. D. Ilge, J. Suhnel, D. Khechinashvili and M. Kaschke, *J. Photochem.*, 1987, **38**, 189.
10 (*a*) S. Abe, K. Uchida, I. Yamazaki and M. Irie, *Langmuir*, 1997, **13**, 5504; (*b*) M. Irie, K. Sakemura, M. Okinaka and K. Uchida, *J. Org. Chem.*, 1995, **60**, 8305; (*c*) M. Frigoli, C. Welch and G. H. Mehl, *J. Am. Chem. Soc.*, 2004, **126**, 15382; (*d*) Y. Chen and D. X. Zeng, *J. Org. Chem.*, 2004, **69**, 5037; (*e*) R. Sasai, H. Itoh, I. Shindachi, T. Shichi and K. Takagi, *Chem. Mater.*, 2001, **13**, 2012; (*f*) S. Shim, T. Joo, S. C. Bae, K. S. Kim and E. Kim, *J. Phys. Chem. A*, 2003, **107**, 8106.
11 (*a*) R. J. Colton, A. M. Guzman and J. W. Rabalais, *Acc. Chem. Res.*, 1978, **11**, 170; (*b*) T. He, Y. Ma, Y. A. Cao, X. L. Hu, H. M. Liu, G. J. Zhang, W. S. Yang and J. N. Yao, *J. Phys. Chem. B*, 2002, **106**, 12670; (*c*) Z. H. Chen, Y. A. Yang, J. B. Qiu and J. N. Yao, *Langmuir*, 2000, **16**, 722; (*d*) S. Sakka, *J. Am. Ceram. Soc.*, 1969, **52**, 69; (*e*) J. N. Yao, K. Hashimoto and A. Fujishima, *Nature*, 1992, **355**, 624.
12 (*a*) M. T. Pope, *Heteropoly and Isopoly Oxometalates*, Springer Verlag, New York, 1983; (*b*) M. T. Pope and A. Müller, *Angew. Chem., Int. Ed. Engl.*, 1991, **30**, 34; (*c*) C. L. Hill, *Chem. Rev.*, 1998, **98**, 1.
13 (*a*) T. Yamase, *Chem. Rev.*, 1998, **98**, 307; (*b*) S. Q. Liu, D. G. Kurth, H. Möhwald and D. Volkmer, *Adv. Mater.*, 2002, **14**, 225; (*c*) A. Chemseddine, C. Sanchez, J. Livage, J. P. Launay and M. Fournier, *Inorg. Chem.*, 1984, **23**, 2609.
14 (*a*) Z. H. Chen, Y. Ma, X. T. Zhang and J. N. Yao, *J. Colloid Interface Sci.*, 2001, **240**, 487; (*b*) Z. H. Chen, B. H. Loo, Y. Ma, Y. W. Cao, A. Ibrahim and J. N. Yao, *ChemPhysChem*, 2004, **5**, 1020; (*c*) T. R. Zhang, W. Feng, R. Lu, C. Y. Bao, X. T. Zhang and Y. Y. Zhao, *Mater. Chem. Phys.*, 2002, **78**, 116; (*d*) G. J. Zhang, H. H. Ke, T. He, D. B. Xiao, Z. H. Chen, W. S. Yang and J. N. Yao, *J. Mater. Res.*, 2004, **19**, 496.
15 (*a*) M. Jiang, E. B. Wang, G. Wei, Z. H. Kang and Z. Li, *New J. Chem.*, 2003, **27**, 1291; (*b*) G. J. Zhang, Z. H. Chen, T. He, H. H. Ke, Y. Ma, K. Shao, W. S. Yang and J. N. Yao, *J. Phys. Chem. B*, 2004, **108**, 6944.
16 T. R. Zhang, W. Feng, R. Lu, C. Y. Bao, T. J. Li and Y. Y. Zhao, *Mater. Chem. Phys.*, 2002, **78**, 380.
17 H. Y. Zhang, L. Xu, E. B. Wang, M. Jiang, A. G. Wu and Z. Li, *Mater. Lett.*, 2003, **57**, 1417.
18 A. Ulman, *An Introduction to Ultrathin Organic Films*, Academic Press, Boston, MA, 1991, p. 442.

19 F. M. Menger and C. A. Littau, *J. Am. Chem. Soc.*, 1993, **115**, 10083.

20 (*a*) M. Sikiric, I. Smit, L. Tusek-Bozic, V. Tomasic and I. Pucic, *Langmuir*, 2003, **19**, 10044; (*b*) R. Oda, I. Huc, J.-C. Homo, B. Heinrich, M. Schmutz and S. Candau, *Langmuir*, 1999, **15**, 2384; (*c*) M.-P. Nieh, S. K. Kumar and R. H. Ferhando, *Langmuir*, 2004, **20**, 9061; (*d*) F. M. Menger and B. N. A. Mbadugha, *J. Am. Chem. Soc.*, 2001, **123**, 875; (*e*) D. Danino, Y. Talmon and R. Zana, *J. Colloid Interface Sci.*, 1997, **185**, 84; (*f*) L. D. Song and M. J. Rosen, *Langmuir*, 1996, **12**, 1149; (*g*) X. Y. Wang, J. B. Wang, Y. L. Wang and H. K. Yan, *Langmuir*, 2004, **20**, 53.

21 (*a*) X. D. Chen, J. B. Wang, N. Shen, Y. H. Luo, M. H. Liu and R. K. Robert, *Langmuir*, 2002, **18**, 6222; (*b*) X. D. Zhai, L. Zhang and M. H. Liu, *J. Phys. Chem. B*, 2004, **108**, 7180; (*c*) M. Jiang, X. D. Zhai and M. H. Liu, *Langmuir*, 2005, **21**, 11128; (*d*) X. D. Zhai and M. H. Liu, *J. Colloid Interface Sci.*, 2006, **295**, 181; (*e*) G. C. Zhang, X. D. Zhai and M. H. Liu, *J. Phys. Chem. B*, 2006, **110**, 10455; (*f*) Jiao and T. M. H. Liu, *Langmuir*, 2006, **22**, 5005.

22 C. R. Deltcheff, M. Fournier, R. Franck and R. Thouvenot, *Inorg. Chem.*, 1983, **22**, 207.

23 T. F. Jiao, G. C. Zhang and M. H. Liu, *J. Phys. Chem. B*, 2007, **111**, 3090.

24 M. Clemente-Leon, C. Mingotaud, C. J. Gomez-Garcia, E. Coronado and P. Delhaes, *Thin Solid Films*, 1998, **327**, 439.

25 M. Jiang, X. D. Zhai and M. H. Liu, *J. Mater. Chem.*, 2007, **17**, 193.

26 (*a*) C. Q. Sun, J. H. Zhao, H. D. Xu, Y. P. Sun, X. Zhang and J. C. Shen, *J. Electroanal. Chem.*, 1997, **435**, 63; (*b*) L. Chen, G. E. Pacey and J. A. Cox, *Electrochim. Acta*, 2001, **46**, 4223; (*c*) M. Sadakane and E. Steckhan, *Chem. Rev.*, 1998, **98**, 219; (*d*) E. Papaconstantinou, Jr and M. T. Pope, *Inorg. Chem.*, 1967, **6**, 1152; (*e*) B. Wang and S. Dong, *J. Electroanal. Chem.*, 1992, **328**, 245.

27 A. P. Brown and F. C. Anson, *Anal. Chem.*, 1977, **49**, 1589.

28 (*a*) G. Ilangovan and K. C. Pillai, *Langmuir*, 1997, **13**, 566; (*b*) J. S. Facci, *Langmuir*, 1987, **3**, 525.

29 (*a*) R. G. Snyder, H. L. Strauss and C. A. Elliger, *J. Phys. Chem.*, 1982, **86**, 5145; (*b*) R. A. MacPhail, H. L. Strauss, R. G. Snyder and C. A. Elliger, *J. Phys. Chem.*, 1984, **88**, 334.

30 G. M. Varga, Jr, E. Papaconstantinou and M. T. Pope, *Inorg. Chem.*, 1970, **9**, 662.